18. Haque T, Furukawa T, Takahashi M, Kinoshita M. Identification of hibernating myocardium by dobutamine stress echocardiography: comparison with thallium-201 reinjection imaging. *Am Heart J* 1995;130:553–563.
19. Nishimura T, Sago M, Kihara K, et al. Fatty acid myocardial imaging using ^{123}I-beta-methyl-iodophenyl pentadecanoic acid (BMIPP): comparison of myocardial perfusion and fatty acid utilization in canine myocardial infarction (occlusion and reperfusion model). *Eur J Nucl Med* 1989;15:341–345.
20. Yamamichi Y, Kusuoka H, Morishita K, et al. Metabolism of iodine-123-BMIPP in perfused rat hearts. *J Nucl Med* 1995;36:1043–1050.
21. Fujibayashi Y, Yonekura Y, Takemura Y, et al. Myocardial accumulation of iodinated beta-methyl-branched fatty acid analog, iodine-125-15-(p-iodophenyl)-3-(R,S)-methylpentadecanoic acid (BMIPP), in relation to ATP concentration. *J Nucl Med* 1990;31:1818–1822.
22. Riendeau D, Guertin D. ATP- and coenzyme A-dependent fatty acid incorporation into proteins of cell-free extracts from mouse tissues. *J Biol Chem* 1986;261:976–981.
23. Saddik M, Gamble J, Witters LA, Lopaschuk GD. Acetyl-CoA carboxylase regulation of fatty acid oxidation in the heart. *J Biol Chem* 1993;268:25836–25845.
24. Matsunari I, Saga T, Taki J, et al. Improved myocardial fatty acid utilization after percutaneous transluminal coronary angioplasty. *J Nucl Med* 1995;36:1605–1607.
25. Takeishi Y, Atsumi H, Fujiwara S, Tomoike H. Delayed metabolic recovery of hibernating myocardium after percutaneous transluminal coronary angioplasty: assessment with iodine-123-beta-methyl-p-iodophenyl-pentadecanoic acid imaging. *J Cardiol* 1996;28:17–25.
26. Dudczak R, Schmoliner R, Angelberger P, Knapp FF, Goodman MM. Structurally modified fatty acids: clinical potential as tracers of metabolism. *Eur J Nucl Med* 1986;12(suppl):S45–S48.
27. Chouraqui P, Maddahi J, Henkin R, Karesh SM, Galie E, Berman DS. Comparison of myocardial imaging with iodine-123-iodophenyl-9-methyl pentadecanoic acid and thallium-201-chloride for assessment of patients with exercise-induced myocardial ischemia. *J Nucl Med* 1991;32:447–452.
28. Kropp J, Jorgens M, Glanzer K, Lunderitz B, Biersack H, Knapp F. Evaluation of ischemia and myocardial viability in patients with coronary artery disease (CAD) with iodine-123 labeled 15-(p-iodophenyl)-3-R,S-methylpentadecanoic acid (BMIPP). *Ann Nucl Med* 1993;7(suppl 2):93–100.
29. Schoonderwoerd K, Broekhoven SS, Hulsmann WC, Stam H. Enhanced lipolysis of myocardial triglycerides during low-flow ischemia and anoxia in the isolated rat heart. *Basic Res Cardiol* 1989;84:165–173.
30. Taki J, Nakajima K, Matsunari I, Bunko H, Takada S, Tonami N. Impairment of regional fatty acid uptake in relation to wall motion and thallium-201 uptake in ischaemic but viable myocardium: assessment with iodine-123-labeled beta-methyl-branched fatty acid. *Eur J Nucl Med* 1995;22:1385–1392.
31. Mori T, Hayakawa M, Hattori K, et al. Exercise beta-methyl iodophenyl acid (BMIPP) and resting thallium delayed single photon emission CT (SPECT) in the assessment of ischemia and viability. *Jpn Circ J* 1996;60:17–26.
32. Kawamoto M, Tamaki N, Yonekura Y, et al. Combined study with I-123 fatty acid and thallium-201 to assess ischemic myocardium: comparison with thallium redistribution and glucose metabolism. *Ann Nucl Med* 1994;8:47–54.
33. Ito T, Tanouchi J, Kato J, et al. Recovery of impaired left ventricular function in patients with acute myocardial infarction is predicted by the discordance in defect size on ^{123}I-BMIPP and ^{201}Tl SPECT images. *Eur J Nucl Med* 1996;23:917–923.

First-Pass Radionuclide Angiography Using Iodine-123 Myocardial Tracers and a Multicrystal Gamma Camera

Eiji Tadamura, Haruhiro Kitano, Takashi Kudoh, Naoya Hattori, Masayuki Inubushi, Kazunobu Nishimura, Izuru Masuda, Hideo Inada, Ryohei Hosokawa, Ryuji Nohara and Junji Konishi

Departments of Nuclear Medicine and Cardiovascular Surgery, Second and Third Divisions, and Department of Internal Medicine, Kyoto University Faculty of Medicine, Kyoto, Japan

The purpose of this study was to validate the accuracy of the assessment of ventricular function by first-pass radionuclide angiography (FPRNA) with ^{123}I myocardial tracers and a multicrystal gamma camera. **Methods:** Left ventricular ejection fraction (LVEF) and right ventricular ejection fraction were measured in 69 patients by FPRNA using ^{123}I myocardial tracers (126 ± 7 MBq) and ^{99m}Tc tracers (541 ± 141 MBq) on a multicrystal gamma camera with a high-sensitivity collimator. For 44 patients, ejection fraction values measured by ^{123}I-FPRNA were compared to those estimated by equilibrium radionuclide angiography (ERNA). Visual wall-motion analysis was also performed to judge clinical acceptability of ^{123}I-FPRNA images for identification of wall-motion abnormality. **Results:** Mean LVEFs (%) estimated by ^{123}I-FPRNA and by ^{99m}Tc-FPRNA were 49.6 ± 13.6 and 49.1 ± 14.1, respectively (nonsignificant p value). An excellent correlation was found between LVEFs estimated by ^{123}I-FPRNA and ^{99m}Tc-FPRNA ($r = 0.96$, s.e.e. = 1.9%). Values of LVEF measured by ^{123}I-FPRNA also demonstrated excellent correlation with those measured by ERNA ($r = 0.95$, s.e.e. = 2.2%). A good correlation was also noted between right ventricular ejection fractions measured by ^{123}I-FPRNA and ^{99m}Tc-FPRNA ($r = 0.72$, s.e.e. = 4.0%). The Spearman rank correlation coefficient between ^{123}I-FPRNA and ERNA wall-motion scores was 0.87 ($n = 135$, $p < 0.001$). **Conclusion:** Resting ventricular function can be reliably measured with ^{123}I-FPRNA in combination with a multicrystal gamma camera. This indicates that the assessment of ventricular function is feasible in conjunction with ^{123}I myocardial imaging without an increase in cost or radiation dose to patients.

Key Words: iodine-123 myocardial tracer; first-pass radionuclide angiography; ejection fraction

J Nucl Med 1998; 39:938–944

Noninvasive assessment of left ventricular (LV) and right ventricular (RV) performance is one of the main goals of nuclear cardiology. Continuous efforts have been made toward this objective, and the several approaches that have been reported include planar equilibrium radionuclide angiography (ERNA) (*1–3*), first-pass radionuclide angiography (FPRNA) (*4–6*), gated blood-pool SPECT (*7–9*) and gated perfusion SPECT (*10–12*). Although there were attempts to use ^{195m}Au (*13*) and ^{191m}Ir (*14*) in FPRNA, ^{99m}Tc agents are now exclusively used in all of these approaches to evaluate ventricular function.

The clinical and investigational usefulness of ^{123}I-labeled radiotracers such as 15-(p-iodophenyl)-3-(R,S)-methylpentadecanoic acid (BMIPP) (*15,16*) and metaiodobenzylguanidine (MIBG) (*17,18*) has now been widely recognized. Mainly because of the longer physical half-life of ^{123}I (13.3 hr) compared to ^{99m}Tc, ^{123}I tracers are injected at limited dose (111–148 MBq), which is disadvantageous for FPRNA. However, we hypothesized that FPRNA using ^{123}I tracers may be feasible if the images are acquired with a multicrystal camera that has higher counting capabilities than the usual single-

Received Jun. 30, 1997; revision accepted Sep. 27, 1997.

For correspondence or reprints contact: Eiji Tadamura, MD, Department of Nuclear Medicine and Diagnostic Imaging, Kyoto University Faculty of Medicine, Shogoin, Sakyo-ku, Kyoto, 606-01, Japan.

TABLE 1
Clinical Characteristics of 72 Patients

Characteristic	Value
Age (yr)	63.2 ± 10.6 (32–82)*
Sex (male-to-female ratio)	44:28
Weight (kg)	58.8 ± 11.1
Height (cm)	160.0 ± 10.0
Heart rate (bpm)	74.4 ± 14.5 (44–101)*
Clinical diagnosis (no. of patients)	
Coronary artery disease	59
Adriamycin cardiomyopathy	5
Diabetes mellitus	5
Chronic heart failure	3

*Numbers in parentheses represent ranges.

crystal gamma camera. Therefore, this study was designed to evaluate the feasibility of the use of ^{123}I tracers in FPRNA acquired with a multicrystal gamma camera in comparison with ^{99m}Tc-FPRNA and ERNA to evaluate ventricular performance.

MATERIALS AND METHODS

This study group consisted of 72 patients who consecutively underwent both ^{123}I myocardial scintigraphy and ^{99m}Tc-FPRNA for clinical indications. The patient profile is shown in Table 1.

Resting FPRNA with ^{123}I tracers (126 ± 7 MBq), including BMIPP (n = 54) and MIBG (n = 18), was conducted before ^{123}I scintigraphy. Informed consent was obtained from each subject before FPRNA. Within a week, every subject also underwent FPRNA using ^{99m}Tc tracers (541 ± 141 MBq), including ^{99m}Tc-human serum albumin (HSA) (n = 46), sestamibi (n = 3), tetrofosmin (n = 3) and free pertechnetate (n = 20), which served as a standard method for the evaluation of ventricular performance in this study. ERNA, if conducted, served as another standard method. Of these 72 combined studies, three studies were excluded because of severe arrhythmia during FPRNA (n = 2) and poor patient positioning (n = 1). Ultimately, 69 combined ^{123}I-FPRNA/^{99m}Tc-FPRNA studies and 44 combined ^{123}I-FPRNA/ERNA studies were analyzed.

FPRNA was acquired in an anterior view (*19,20*) with a multicrystal gamma camera (model SIM-400; Scinticor, Milwaukee, WI; maximum counting rate = 1000 kcps with 20% loss at 780 kcps) (*21*), equipped with a high-sensitivity, parallel-hole collimator interfaced with a microcomputer (Macintosh Quadra 950, Apple, Inc.). The matrix size was 20 × 20 pixels, with center-to-center pixel spacing of 10 mm. Data were collected with intervals of 50 msec (*22*). A 30% window was centered on the 140-keV photon peak for ^{99m}Tc studies and on the 159-keV peak for ^{123}I studies. An 18- or 20-gauge indwelling polytetrafluoroethylene catheter was placed into the antecubital vein of the right arm and connected to a saline-filled large-bore tubing ending with a three-way stopcock. Iodine-123 myocardial tracer was slowly injected into the tubing through the lateral opening of the stopcock, preceded and followed by a small air bubble. Bolus injection was then performed with a steady and firm injection of 20 ml of normal saline through the straight opening of the stopcock. The total acquisition time was approximately 30 sec for each first-pass study. Within a week of this FPRNA study, during which time the patients were in stable condition, another FPRNA study was performed using ^{99m}Tc tracer in a similar fashion.

Equilibrium radionuclide angiography was also performed when ^{99m}Tc-HSA was used in FPRNA studies. Approximately 5 min after the end of FPRNA using ^{99m}Tc-HSA, ERNA images were acquired in the "best septal" left anterior oblique (LAO) and anterior views using a single-crystal gamma camera equipped with a low-energy, general-purpose collimator (Optima; General Electric Medical Systems, Milwaukee, WI). To attain the best ventricular separation, we used SPECT images obtained in advance as a reference. The LAO study from which LVEF was determined contained a total of at least 5 million counts. Images were recorded in frame mode (20 frames/cycle).

Radionuclide Angiography Analysis

FPRNA data were stored in a Macintosh computer and processed with commercially available software as described previously (*23–26*). In brief, raw data were temporally smoothed and corrected for detector nonuniformity and deadtime. After assignment of a region of interest (ROI) over the left ventricle, a histogram of serial counts as a function of time was created to identify the end-diastolic and end-systolic frames. Only cycles with > 70% of the maximal end-diastolic activity in the end-diastolic frame were included in the analysis (*20,27*). The same ROI as the end-diastolic LV ROI was applied to the lung images just before the LV phase and used for measurement of the background activity for LV analysis. A background-corrected representative LV cycle was generated from accepted heartbeats within the LV phase. Data processing for the RV was almost the same as that for the LV, except that the background was not subtracted for the RV. Valvular planes at the inflow or outflow tract of the ventricle were determined with the help of phase images. A single end-diastolic ROI was used to calculate the RVEF. LVEF and RVEF were calculated with a count-based ratio method (*28,29*).

In ERNA studies, LVEF was calculated on the LAO images. LVEF was calculated with standard, commercially available, semi-automated software. LVEF was calculated by the standard counting rate-based, background-corrected formula.

LVEF calculations in different methods were conducted by separate observers without knowledge of other radionuclide or clinical data. RVEF was measured only from ^{123}I-FPRNA and ^{99m}Tc-FPRNA images because ERNA is not considered a reference standard for calculation of RVEF (*30–32*).

Wall-Motion Evaluation

Regional wall motion was visually analyzed on a dynamic continuous display by two observers who had no knowledge of other patient data, and visual interpretation was determined by consensus. The anterior view of the LV in FPRNA and ERNA images was subdivided into three segments (anterior, apical and inferior wall). A four-point scoring scale was used: 3 = normal; 2 = mild hypokinesia; 1 = severe hypokinesia; and 0 = akinesia or dyskinesis (*23*).

Statistical Analysis

Data are expressed as mean ± s.d. The statistical significance of difference in mean values between paired data were analyzed with the paired Student's t-test. Linear regression analysis was used to compare ejection fraction values obtained by the different methods. Systemic error and the degree of agreement were assessed according to the method of Bland and Altman (*33,34*). Evaluation of agreement between wall-motion scores was performed using Spearman's rank correlation and chi-square analysis of contingency tables in which scores were paired for each territory. A p value of <0.05 was considered to indicate statistical significance.

RESULTS

Time-activity curves of the RV and LV in ^{123}I-FPRNA of a representative case are shown in Figure 1. The end-diastolic and end-systolic phases could be clearly identified.

The mean FWHM values of the time-activity curve generated using a superior vena cava ROI in ^{123}I-FPRNA and ^{99m}Tc-

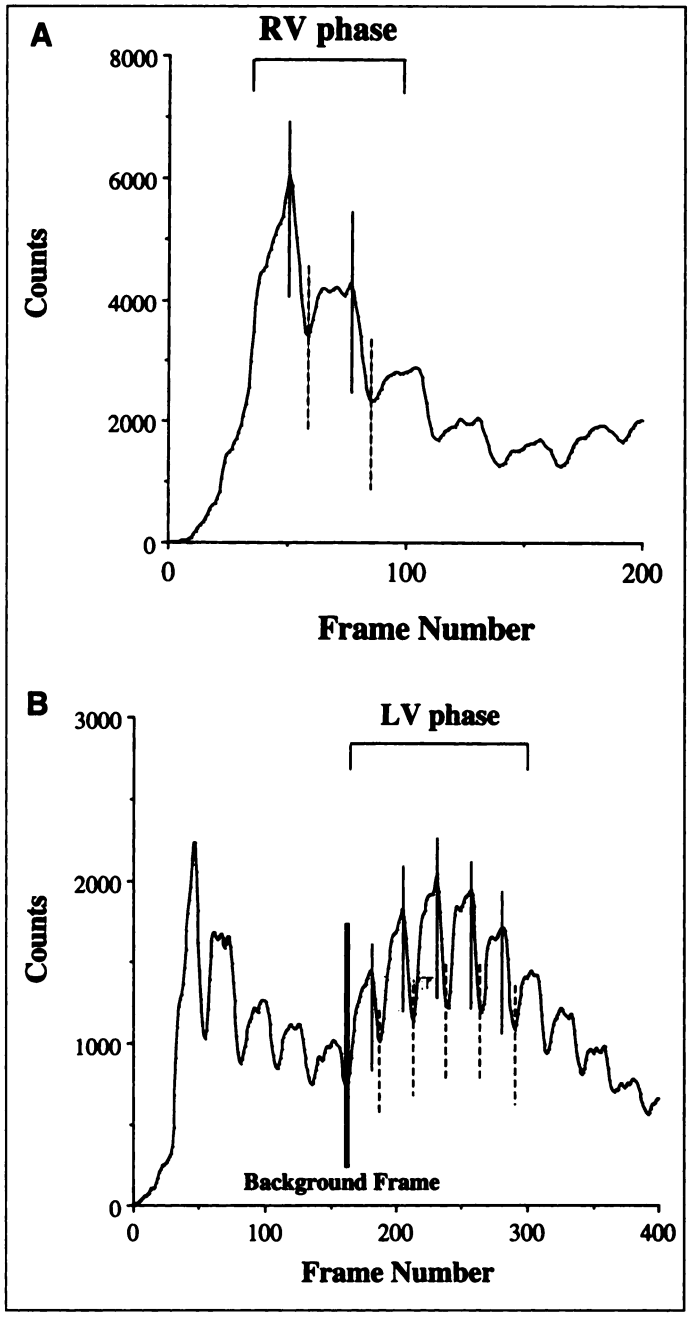

FIGURE 1. Typical time-activity curves of RV (A) and LV (B) ROIs in ^{123}I-FPRNA. Dotted lines = end-systolic frame; solid lines = end-diastolic frame.

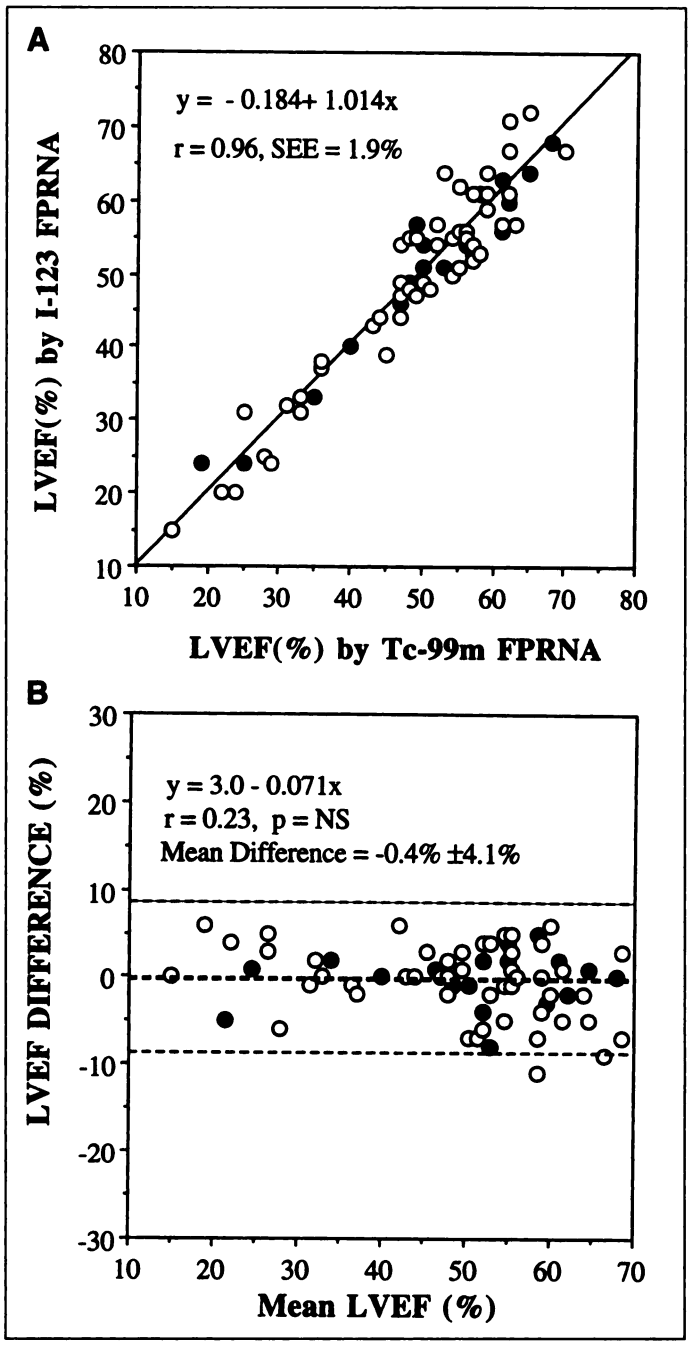

FIGURE 2. Scatterplots (A) and Bland–Altman plots (B) are shown for LVEF obtained with ^{123}I-FPRNA and ^{99m}Tc-FPRNA. ● = MIBG; ○ = BMIPP.

FPRNA were 797 ± 247 msec and 787 ± 216 msec, respectively (nonsignificant p value).

A bolus of ^{123}I myocardial tracers result in an average whole field-of-view counting rate of 174,201 ± 18,644 Hz (range 144,000–215,000 Hz) during the RV phase and 130,102 ± 15,005 Hz (range 96,000–161,000 Hz) during the LV phase. The mean background-corrected end-diastolic counts in the LV representative cycle in ^{123}I-FPRNA and ^{99m}Tc-FPRNA studies were 4,958 ± 1,825 (range 2,730–12,523) and 20,849 ± 8,260 (range 7,672–39,168), respectively ($p < 0.001$).

Left Ventricular Ejection Fraction

The mean LVEF values (%) estimated by ^{123}I-FPRNA and ^{99m}Tc-FPRNA were 49.6 ± 13.6 and 49.1 ± 14.1, respectively (nonsignificant p value). Values of LVEF by these two methods were linearly well correlated with each other (r = 0.96, s.e.e. = 1.9%) (Fig. 2A). Those estimated by ^{123}I-FPRNA and ERNA were also linearly well correlated with each other (r = 0.95, s.e.e. = 2.2%) (Fig. 3A). Bland–Altman analysis revealed no significant degree of systematic measurement bias (Figs. 2B and 3B).

Right Ventricular Ejection Fraction

The mean RVEF values (%) estimated by ^{123}I-FPRNA and ^{99m}Tc-FPRNA were 41.7 ± 8.2 and 41.2 ± 7.8, respectively (nonsignificant p value). Values of RVEF by these two methods were linearly correlated with each other (r = 0.72, s.e.e. = 4.0%) (Fig. 4A). Bland–Altman analysis disclosed no significant directional change in this numeric bias with the RVEF values (Fig. 4B).

Left Ventricular Regional Wall Motion

An example of ^{123}I-FPRNA ventriculograms is shown in Figure 5. The number of segments rated at each visual wall-motion score for ^{123}I-FPRNA and ^{99m}Tc-FPRNA images is

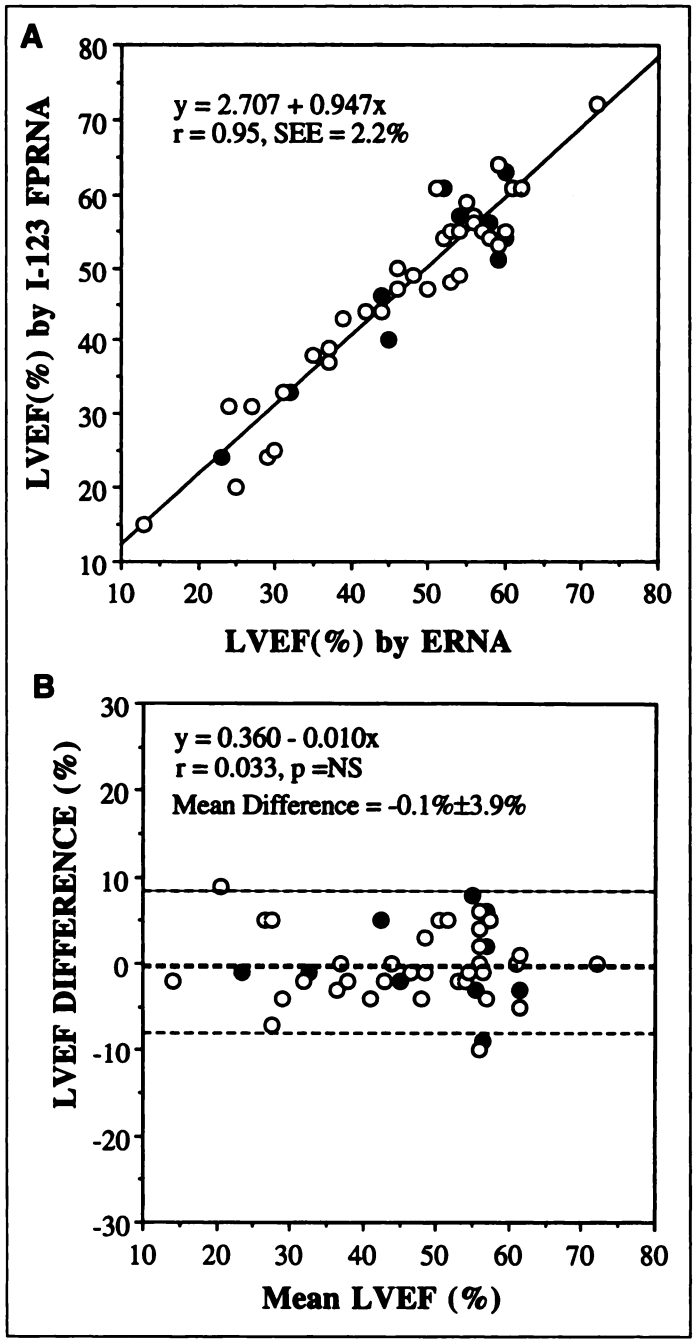

FIGURE 3. Scatterplots (A) and Bland–Altman plots (B) are shown for LVEF obtained with ^{123}I-FPRNA and ERNA. ● = MIBG; ○ = BMIPP.

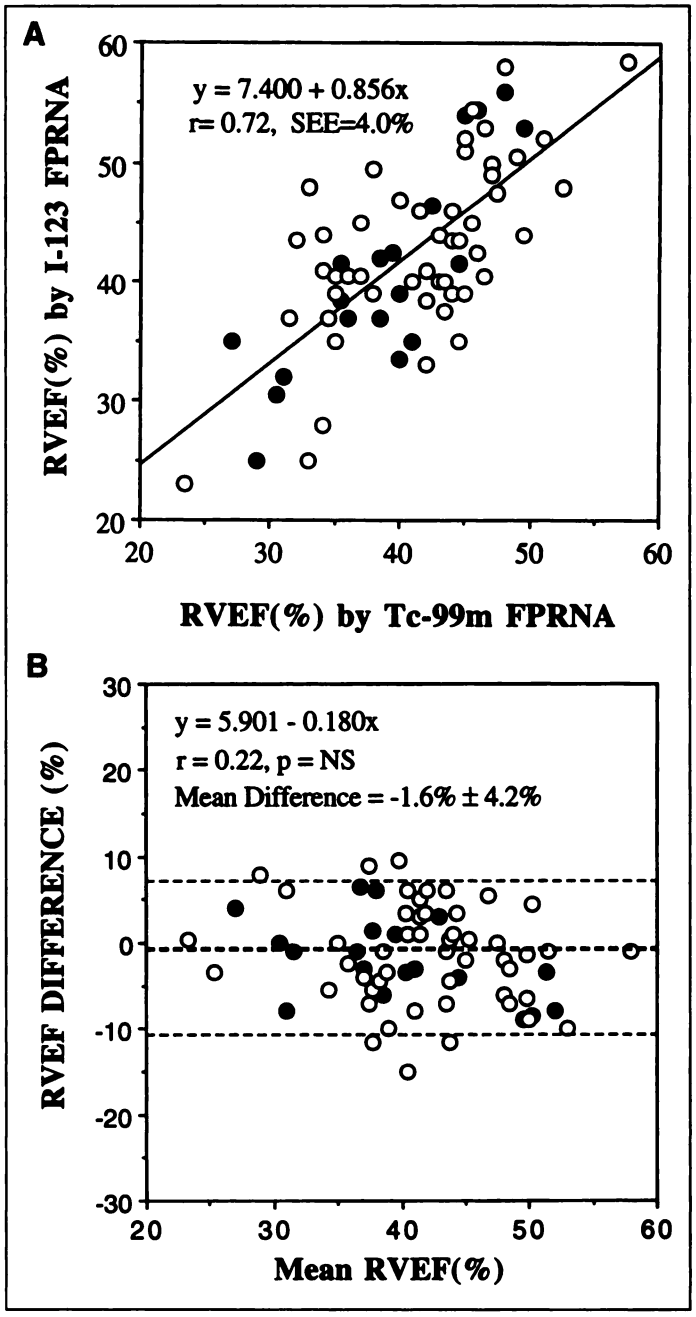

FIGURE 4. Scatterplots (A) and Bland–Altman plots (B) are shown for RVEF obtained with ^{123}I-FPRNA and ^{99m}Tc-FPRNA. ● = MIBG; ○ = BMIPP.

shown in Table 2. For these data, the chi-square was 436.3 for 9 degrees of freedom ($p < 0.001$). Two-hundred-seven segments were judged, for which the Spearman rank correlation test yielded $r_s = 0.93$ ($p < 0.001$). The contingency table of visual wall-motion scores of ^{123}I-FPRNA against those of ERNA is presented in Table 3. The chi-square was 194.7 for 9 degrees of freedom ($p < 0.001$). A Spearman rank correlation between ^{123}I-FPRNA and ERNA wall-motion scores gave a coefficient of 0.87 ($n = 135$, $p < 0.001$).

DISCUSSION

These data demonstrated that the resting LVEF values estimated by ^{123}I-FPRNA correlate well with those obtained with established standard methods, including ^{99m}Tc-FPRNA and ERNA. A good correlation was also noted between RVEF measured by ^{123}I-FPRNA and ^{99m}Tc-FPRNA, although the correlation was not as high as that in LVEF estimates. A high degree of correlation was found between the wall-motion scores of ^{123}I-FPRNA and those of ^{99m}Tc-FPRNA or ERNA. These results indicate that ^{123}I-FPRNA acquired with a multicrystal gamma camera is a reliable new approach of evaluating ventricular performance.

Count Statistics

Nichols et al. (*35*) suggested that LVEF estimation is hampered by the difficulty in the delineation of end-diastolic and end-systolic regions with too few counts. In this study, however, we did not encounter any difficulty in determining the end-diastolic and end-systolic regions. In fact, the mean background-corrected LV end-diastolic count was 4958 ± 1825 (range 2730–12,523) in ^{123}I-FPRNA, which is well above the value (2000) recommended by Wackers et al. (*36*). Port (*37*) suggested that count requirements for high-quality first-pass data exceed 200,000 Hz. Our data were less than this value. However, the average counting rate of 174,201 Hz in our study

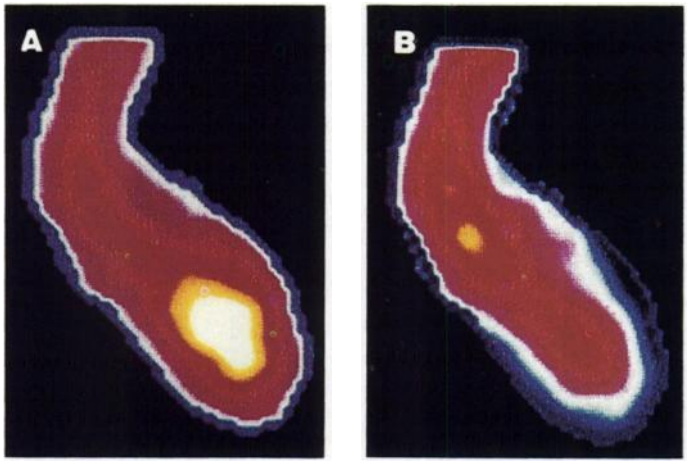

FIGURE 5. Typical LV end-diastolic (A) and end-systolic (B) phases of representative cycles obtained from ^{123}I-FPRNA studies in a patient with inferior infarction. Severe hypokinesis in the inferior wall can be identified by ^{123}I-FPRNA.

is still above the value obtained with a high-counting rate single-crystal gamma camera and approximately 25 mCi of ^{99m}Tc agents (*28,38*). These indicate that the count statistics are satisfactory even when ^{123}I tracers are used in FPRNA. Moreover, the high correlation found between the wall-motion scores of ^{123}I-FPRNA and ^{99m}Tc-FPRNA or ERNA shows that the image quality is adequate for visual assessment of regional wall motion (Fig. 5).

Right Ventricular Ejection Fraction Measurements

The correlation of RVEF estimates between ^{123}I-FPRNA and ^{99m}Tc-FPRNA ($r = 0.72$) was not as high as that of LVEF estimates. The reason is unclear. The RV phase of the initial transit of the radionuclide tracer is shorter than the LV phase. Accepted beats for the RV phase were fewer than those for the LV phase (Fig. 1), which may have caused an error. In addition, atrial overlap also causes errors. To separate the right ventricle and atrium, the right anterior oblique (RAO) view is usually used in FPRNA. In this study, however, we performed FPRNA in the anterior view because we thought that the RAO view would result in poor count statistics if low-activity doses of ^{123}I tracers were used. Our results indicated that the count statistics were adequate even when a small dose of ^{123}I tracers (126 ± 7 MBq) was used. Therefore, FPRNA in the RAO view might improve the correlation coefficient for the assessment of RV performance.

Comparison with Other Radionuclide Techniques to Evaluate Left Ventricular Performance

Of the several techniques of evaluating ventricular performance using nuclear cardiovascular methods cited above (*1–12*), each has distinctive advantages and disadvantages. Recently, ERNA using blood-pool agents has been replaced by FPRNA or gated perfusion SPECT using ^{99m}Tc perfusion tracer because simultaneous assessment of perfusion and function is feasible with a single injection of radiotracer in the latter approaches (*39,40*). This study is unique in two ways. First, we used ^{123}I tracers in FPRNA. Second, we also used tracers other than perfusion or blood-pool agents to assess ventricular performance.

TABLE 2
Contingency Table of Iodine-123 First-Pass Visual Wall-Motion Scores Against Technetium-99m First-Pass Visual Wall-Motion Scores

	^{123}I scores			
^{99m}Tc scores	3	2	1	0
3	127	10	0	0
2	5	22	2	0
1	0	1	10	0
0	0	0	1	29

TABLE 3
Contingency Table of Iodine-123 First-Pass Visual Wall-Motion Scores Against Equilibrium Visual Wall-Motion Scores

	^{123}I scores			
Equilibrium scores	3	2	1	0
3	65	4	0	0
2	16	13	0	0
1	1	1	10	1
0	0	0	7	17

Availability of the Multicrystal Gamma Camera and Iodine-123 Myocardial Tracers

Because the clinical application of a multicrystal gamma camera is mainly limited to FPRNA using ^{99m}Tc tracers, it is unavailable in many institutions. There have been attempts to perform FPRNA using a single-crystal gamma camera (*19,35*). They use an ultra-high-sensitivity collimator that is different from the high-resolution collimator typically used for gated ^{99m}Tc perfusion SPECT studies. Therefore, it requires changing collimators between the functional and perfusion studies, which is troublesome and impractical in clinical settings. Accordingly, a multicrystal gamma camera is best suited for ^{99m}Tc-FPRNA, especially in an exercise study, and its availability is increasing (*23–28,31*). Reportedly, a multicrystal gamma camera can be also used for upright SPECT when it is coupled to a rotating chair (*39*).

The availability of ^{123}I myocardial tracers is also limited especially in the U.S. The cost of ^{123}I studies compared to other radionuclides such as ^{99m}Tc-sestamibi and thallium may be a problem. However, a clinical trial of ^{123}I-phenylpentadecanoic acid (IPPA) was recently performed in the U.S., and its utility was reported (*41*). Thus, ^{123}I myocardial tracers, including MIBG, BMIPP and IPPA, may become more available throughout the world.

This study shows the feasibility of the use of ^{123}I tracers in FPRNA to assess ventricular performance, which will likely expand the clinical applicability of the multicrystal gamma camera as well as ^{123}I myocardial tracers.

Clinical Implications

The value of BMIPP and MIBG scintigraphy has been widely recognized. Assessment of myocardial viability in combination with flow tracers such as thallium is reported to be feasible in ischemic coronary artery disease (*15,16,42*), and its prognostic values were also reported (*43*). Additionally, clinical and investigational usefulness of BMIPP is also shown in patients with hypertrophic cardiomyopathy (*44,45*). Similarly, MIBG has been reported to have prognostic potential in patients with congestive heart failure (*17,18*). Its utility has also been suggested in patients with diabetes mellitus (*46*). Thus, ^{123}I myocardial tracers have been recognized to provide important sympathetic or metabolic information other than myocardial perfusion. Such information is necessary for the elucidation of myocardial pathophysiology in various cardiac diseases and the clinical evaluation of prognosis.

On the other hand, thallium is still widely used as a myocardial perfusion agent, mainly because of its long history and its well-established utility in evaluating myocardial viabil-

ity (*47*). The present results indicate that the assessment of ventricular performance using ^{123}I-FPRNA is feasible even though ^{99m}Tc agents are not used as the perfusion tracer. Moreover, in certain myocardial diseases (*17,18,45,46*), the evaluation of cardiac sympathetic function or free fatty acid utilization is more important than the assessment of myocardial perfusion. Even in this context, the assessment of resting ventricular performance is feasible as a secondary objective of ^{123}I myocardial scintigraphy. This would obviate the use of ^{99m}Tc tracers to assess ventricular performance, leading to simplification of cardiovascular nuclear studies and also contributing to the reduction of the radiation doses to patients. Moreover, this approach would provide an increased amount of clinically valuable information with minimal or no increase in cost, which is important in the current cost-conscious environment. We believe that such additional information in combination with the data obtained with ^{123}I myocardial scintigraphy would greatly facilitate decisions in patient management.

Study Limitations

The physical constitution of the average Japanese person is smaller than that of the average Western person (Table 1). Therefore, further studies, including those with larger subjects, are warranted to validate the use of ^{123}I myocardial tracers for FPRNA. However, the limited dose of ^{123}I tracers used in the current study would not cause a substantial error in the evaluation of ventricular performance because all data were acquired during the initial transit of a radionuclide bolus through the central circulation before the tracer was distributed throughout the whole body. Moreover, the use of ^{123}I is advantageous in terms of tissue attenuation because it has a high-energy peak (159 keV). Even in obese patients or in women with large breasts, cardiac ventricular performance can be reliably assessed without a significant increase of the injected dose.

CONCLUSION

The current study demonstrated that resting global and regional cardiac function can be assessed with ^{123}I-FPRNA in conjunction with a multicrystal gamma camera. Thus, ventricular performance can be assessed with ^{123}I myocardial scintigraphy with only a single injection of radiotracer. This may lead to comprehensive assessment of various cardiac diseases. We believe that the addition of FPRNA before ^{123}I myocardial scintigraphy has the potential to augment diagnostic and prognostic accuracy, without an increase in cost or radiation dose to patients.

ACKNOWLEDGMENTS

We thank Emiko Komori, RT, and Toru Fujita, RT, at Kyoto University Hospital for their excellent technical assistance. We also thank Nisho Iwai Co., Ltd., for providing the SIM-400 system and a microcomputer.

REFERENCES

1. Strauss HW, Zaret BL, Hurley PJ, Natarajan TK, Pitt B. A scintigraphic method for measuring left ventricular ejection fraction in man without cardiac catheterization. *Am J Cardiol* 1971;28:575–580.
2. Borer JS, Bacharach SL, Green MV, et al. Real-time radionuclide cineangiography in the noninvasive evaluation of global and regional left ventricular function at rest and during exercise in patients with coronary-artery disease. *N Engl J Med* 1977;296:839–844.
3. Wackers FJT, Berger HJ, Johnstone DE, et al. Multiple gated cardiac blood-pool imaging for left ventricular ejection fraction: validation of the technique and assessment of variability. *Am J Cardiol* 1979;43:1159–1166.
4. Burke G, Halko A, Peskin G. Determination of cardiac output by radionuclide angiography and the image intensifier scintillation camera. *J Nucl Med* 1971;12:112–116.
5. Van Dyle D, Anger HO, Sullivan RW, et al. Cardiac evaluation from radioisotope dynamics. *J Nucl Med* 1972;13:484–492.
6. DePuey EG, Salensky H, Melancon S, Nichols KJ. Simultaneous biplane first-pass radionuclide angiocardiography using a scintillation camera with two perpendicular detectors. *J Nucl Med* 1994;35:1593–1601.
7. Cerqueria MD, Harp GD, Ritchie JL. Quantitative gated blood-pool tomographic assessment of regional ejection fraction: definition of normal limits. *J Am Coll Cardiol* 1992;20:934–941.
8. Bartlett ML, Srinivasan G, Barker WC, Kitsiou AN, Dilsizian V, Bacharach SL. Left ventricular ejection fraction: comparison of results from planar and SPECT gated blood-pool studies. *J Nucl Med* 1996;37:1795–1799.
9. Chin BB, Bloomgarden DC, Xia W, et al. Right and left ventricular volume and ejection fraction by tomographic gated blood-pool scintigraphy. *J Nucl Med* 1997;38:942–948.
10. DePuey EG, Nichols K, Dobrinsky C. Left ventricular ejection fraction assessed from gated ^{99m}Tc-sestamibi SPECT. *J Nucl Med* 1993;34:1871–1876.
11. Germano G, Kiat H, Kavanaugh PB, et al. Automatic quantification of ejection fraction from gated myocardial perfusion SPECT. *J Nucl Med* 1995;38:2138–2147.
12. Williams KA, Taillon LA. Left ventricular function in patients with coronary artery disease assessed by gated tomographic myocardial perfusion images: comparison with assessment of by contrast ventriculography and first-pass radionuclide angiography. *J Am Coll Cardiol* 1996;27:173–181.
13. Wackers FJ, Stein R, Pytlik L, et al. Gold-195m for serial first pass radionuclide angiocardiography during upright exercise in patients with coronary artery disease. *J Am Coll Cardiol* 1983;2:497–505.
14. Heller GV, Treves ST, Parker JA, et al. Comparison of ultrashort-lived iridium-191m with technetium-99m for first pass radionuclide angiocardiographic evaluation of right and left ventricular function in adults. *J Am Coll Cardiol* 1986;7:1295–1302.
15. Knapp FF, Franken P, Kropp J. Cardiac SPECT with iodine-123-labeled fatty acids: evaluation of myocardial viability with BMIPP. *J Nucl Med* 1995;36:1022–1030.
16. Knapp FF, Kropp J. Iodine-123-labeled fatty acids for myocardial single-photon emission tomography: current status and future perspectives. *Eur J Nucl Med* 1995;22:361–381.
17. Henderson EB, Kahn JK, Corbett JR, et al. Abnormal iodine-123 metaiodobenzylguanidine myocardial washout and distribution may reflect myocardial adrenergic derangement in patients with congestive cardiomyopathy. *Circulation* 1988;78:1192–1199.
18. Merlet P, Valette H, Dubois Rande JL, et al. Prognostic value of cardiac metaiodobenzylguanidine imaging in patients with heart failure. *J Nucl Med* 1992;33:471–477.
19. Esquerré JP, Coca FJ, Gantet P, Ouhayoun E. Feasibility of first-pass radionuclide angiography with a 10-mCi technetium bolus using a single-crystal digital gamma camera: implications for technetium-sestamibi single-day protocols. *Eur J Nucl Med* 1995;22:521–527.
20. Di Salvo TG, Mathier M, Semigran MJ, Dec GW. Preserved right ventricular ejection fraction predicts exercise capacity and survival in advanced heart failure. *J Am Coll Cardiol* 1995;25:1143–1153.
21. DePuey EG, Berger HJ. Evaluation of cardiac function using first pass radionuclide angiocardiography. In: Adam WE, ed. *Handbook of nuclear medicine*, vol. 2. New York: Gustav Fisher Verlag; 1993:103–126.
22. Schelbert HR, Verba JW, Johnson AD, et al. Nontraumatic determination of left ventricular ejection fraction by radionuclide angiocardiography. *Circulation* 1975;51:902–909.
23. Takahashi N, Tamaki N, Tadamura E, et al. Combined assessment of regional perfusion and wall motion in patients with coronary artery disease with technetium 99m tetrofosmin. *J Nucl Cardiol* 1994;1:29–38.
24. Friedman JD, Berman DS, Kiat H, et al. Rest and treadmill exercise first-pass radionuclide ventriculography: validation of left ventricular ejection fraction measurements. *J Nucl Cardiol* 1994;1:382–388.
25. Kondo C, Nakagawa M, Kusakabe K, Momma K. Left ventricular dysfunction on exercise long term after total repair of teratology of Fallot. *Circulation* 1995;92(suppl 2):II-250–II-255.
26. Gallik DM, Obermueller SD, Swarna US, Guidry GW, Mahmarian JJ, Verani MS. Simultaneous assessment of myocardial perfusion and left ventricular function during transient coronary occlusion. *J Am Coll Cardiol* 1995;25:1529–1538.
27. Borges-Neto S, Coleman RE, Jones RH. Perfusion and function at rest and treadmill exercise using technetium-99m-sestamibi: comparison of 1- and 2-day protocols in normal volunteers. *J Nucl Med* 1990;31:1128–1132.
28. Gal RA, Grenier RP, Port SC, Dymond DS, Schmidt DH. Left ventricular volume calculation using a count-based ratio method applied to first-pass radionuclide angiography. *J Nucl Med* 1992;33:2124–2132.
29. Massardo T, Gal R, Grenier RP, Schmidt DH, Port SC. Left ventricular volume calculation using a count based ratio method applied to multigated radionuclide angiography. *J Nucl Med* 1990;31:450–456.
30. Rezai K, Weiss R, Stanford W, Preslar J, Marcus M, Kirchner P. Relative accuracy of three scintigraphic methods for determination of right ventricular ejection fraction: a correlative study with ultrafast CT. *J Nucl Med* 1990;32:429–435.
31. Johnson LL, Lawson MA, Blackwell GG, Tauxe EL, Russel K, Dell'Italia LJ. Optimizing the method to calculate right ventricular fraction from first-pass data acquired with a multicrystal camera. *J Nucl Cardiol* 1995;2:372–379.
32. Schulman D. Assessment of the right ventricle with radionuclide techniques. *J Nucl Cardiol* 1996;3:253–264.
33. Bland JM, Altman DG. Statistical methods for assessing agreement between two methods of clinical measurement. *Lancet* 1986;1:307–310.
34. Bland JM, Altman DG. A note on the use of the intraclass correlation coefficient on the evaluation of agreement between two methods of measurement. *Comput Biol Med* 1990;20:337–340.
35. Nichols K, DePuey EG, Gooneratne N, Salensky H, Friedman M, Cochoff S. First-pass ventricular ejection fraction using a single-crystal nuclear camera. *J Nucl Med* 1994;35:1292–1300.
36. Wackers FJT, Sinusas A, Saari MA, Mattera JA. Is list mode ECG-gated first pass

LVEF accurate using a single crystal gamma camera? Implications for ^{99m}Tc-labeled perfusion imaging agents [Abstract]. *J Nucl Med* 1991;32(suppl):939.
37. Port SC. Recent advances in first-pass radionuclide angiography. *Cardiol Clin* 1994;12:359–372.
38. Gal R, Grenier RP, Carpenter J, Schmidt DH, Port SC. High counting rate first-pass radionuclide angiography using a digital gamma camera. *J Nucl Med* 1986;27:198–206.
39. Port SC. The first pass ventricular function study: why now? *J Nucl Med* 1994;35: 1301–1302.
40. Berman DS, Germano G, Kiat H, Friedman J. Simultaneous perfusion/function imaging. *J Nucl Cardiol* 1995;3:271–273.
41. Hansen CL, Heo J, Oliner C, Van Decker W, Iskandrian AS. Prediction of improvement in left ventricular function with iodine-123-IPPA after coronary revascularization. *J Nucl Med* 1995;36:1987–1993.
42. Tamaki N, Tadamura E, Kawamoto M, et al. Decreased uptake of iodinated branched fatty acid analog indicates metabolic alterations in ischemic myocardium. *J Nucl Med* 1995;36:1974–1980.
43. Tamaki N, Tadamura E, Kudoh T, et al. Prognostic value of iodine-123 labeled BMIPP fatty acid analog imaging in patients with myocardial infarction. *Eur J Nucl Med* 1996;23:272–279.
44. Tadamura E, Kudoh T, Hattori N, et al. Impairment of BMIPP uptake precedes abnormalities in oxygen and glucose metabolism in hypertrophic cardiomyopathy. *J Nucl Med* 1998:39;390–396.
45. Nishimura T, Nagata S, Uehara T, et al. Prognosis of hypertrophic cardiomyopathy: assessment by iodine-123 BMIPP (beta-methyl-p-(I-123)iodophenyl pentadecanoic acid) myocardial single photon emission CT. *Ann Nucl Med* 1996;10:71–78.
46. Kreiner G, Wolzt M, Fasching P, et al. Myocardial m-[^{123}I] iodobenzylguanidine scintigraphy for the assessment of adrenergic cardiac innervation in patients with IDDM. Comparison with cardiovascular reflex tests and relationship to left ventricular function. *Diabetes* 1995;44:543–549.
47. Dilsizian V, Rocco TP, Freedman NM, Leon MB, Bonow RO. Enhanced detection of ischemic but viable myocardium by the reinjection of thallium after stress-redistribution imaging. *N Engl J Med* 1990;323:141–146.

Adenosine Receptor Blockade Enhances Myocardial Stunning Without a Sustained Effect on Fluorine-18-FDG Uptake Postreperfusion

Edward O. McFalls, Douglas Baldwin, David Marx, Diane Jaimes, Peggy Fashingbauer and Herbert B. Ward
Division of Cardiology, VA Medical Center, University of Minnesota, Minneapolis, Minnesota

The aim of this study was to determine whether adenosine receptor blockade before ischemia would enhance the degree of stunning and induce a sustained decrease in glucose uptake after reperfusion. **Methods:** Stunning was induced in 14 anesthetized swine by partially occluding the left anterior descending artery (LAD) for 20 min (> 80% flow reduction). Seven animals were pretreated with the nonspecific adenosine receptor blocker 8-phenyltheophylline (8-PT; 5 mg/kg), which decreased reactive hyperemia by an average of 38%. Myocardial glucose uptake was assessed 1 hr following reperfusion with PET and the glucose analog ^{18}F-fluorodeoxyglucose (FDG). **Results:** Before ischemia, systolic shortening in the LAD region was 15% ± 6% in the control group and 16% ± 4% in the 8-PT group and in both groups was reduced to − 1% ± 2% during ischemia. After reperfusion, systolic shortening was 7% ± 3% in the control group and 2% ± 3% in the 8-PT group ($p < 0.05$). Myocardial oxygen consumption before ischemia was 4.58 ± 3.03 μmol/min/g in the control group and 4.44 ± 1.83 μmol/min/g in the 8-PT group (ns) and neither were different after reperfusion. In the postischemic LAD region, myocardial glucose uptake was 0.18 ± 0.15 μmol/min/g in the control group and was similar to that of the 8-PT group (0.17 ± 0.08 μmol/min/g; ns). **Conclusion:** The nonspecific adenosine blocker 8-PT enhanced the degree of stunning when given before ischemia but did not induce a sustained effect on myocardial glucose uptake after reperfusion.

Key Words: PET; fluorine-18-fluorodexoyglucose; stunning; adenosine; glucose; metabolism; reperfusion injury

J Nucl Med 1998; 39:944–949

Exogenous adenosine protects the myocardium from ischemic injury. When administered before prolonged periods of ischemia, it prevents necrosis by initiating a preconditioning cascade through the A_1 receptor (*1*). When administered during early reperfusion, it restores perfusion and prevents "no-reflow," potentially through the A_2 receptor (*2,3*). During brief periods of ischemia, augmenting endogenous levels of adenosine also may be protective by attenuating the degree of stunning (*4–7*). Although the mechanism of this observation is complex, one possibility is that adenosine receptor stimulation could alter metabolism favorably, either during ischemia by decreasing oxygen demands (*8*) or after reperfusion, by increasing glucose uptake (*9*). Enhanced glucose uptake during early reperfusion may be protective by maintaining calcium homeostasis (*10*) and this in turn may be modulated by adenosine (*9,11–13*). Accordingly, the aim of this study was to determine whether 8-phenyltheophylline (8-PT), a nonselective adenosine receptor blocker, enhances the degree of stunning while decreasing glucose uptake postreperfusion. Anesthetized swine were used for these studies and myocardial glucose uptake was measured by PET and the glucose analog ^{18}F-fluorodeoxyglucose (FDG).

MATERIALS AND METHODS

This study was performed under the guidance of the Animal Care Committee at the VA Medical Center, Minneapolis, MN and conforms with U.S. National Institutes of Health Publication No. 85-23 (*14*).

Animal Preparation

Fasted swine of either sex (30–38 kg) were sedated with ketamine (20 mg/kg; intramuscular) and pentobarbitone (10 mg/kg; intravenous) infused into an ear vein. They were intubated, connected to a respirator and ventilated with oxygen-enriched air to maintain normal arterial pH (7.35–7.45), pCO_2 (35–45 mm Hg) and pO_2 (>100 mm Hg). The left external jugular vein and internal carotid artery were exposed and cannulated with 7F catheters. Anesthesia was initiated with a bolus of alpha chloralose (150 mg/kg; intravenous) supplemented with an infusion of sodium pentobarbitone (5 mg/kg/hr). The right femoral artery was exposed and cannulated with a 7F catheter and used for blood sampling and blood pressure measurement.

After administration of succinyl choline (0.25 mg; intravenous), a midline sternotomy was performed and the heart was suspended

Received Jun. 16, 1997; revision accepted Oct. 13, 1997.
For correspondence or reprints contact: Edward O. McFalls MD, PhD, Division of Cardiology, VA Medical Center, 1 Veterans Dr., Minneapolis, MN 55417.